

# Dynamic structure function of two interacting atoms in 1D

David Ledesma,<sup>1</sup> Alejandro Romero-Ros,<sup>1,2</sup> Artur Polls,<sup>1,3</sup> and Bruno Juliá-Díaz<sup>1,3,4</sup>

<sup>1</sup>*Departament de Física Quàntica i Astrofísica,  
Facultat de Física, Universitat de Barcelona, E-08028 Barcelona, Spain*

<sup>2</sup>*Zentrum für Optische Quantentechnologien,  
Universität Hamburg, Luruper Chaussee 149, 22761 Hamburg, Germany*

<sup>3</sup>*Institut de Ciències del Cosmos, Universitat de Barcelona,  
IEEC-UB, Martí i Franquès 1, E-08028 Barcelona, Spain*

<sup>4</sup>*ICFO-Institut de Ciències Fotòniques, Parc Mediterrani de la Tecnologia, E-08860 Barcelona, Spain*

We consider two atoms trapped in a one-dimensional harmonic oscillator potential interacting through a contact interaction. We study the transition from the non-interacting to the strongly interacting Tonks-Girardeau state, as the interaction is varied from zero to infinitely large repulsive values. The dynamic structure function is computed by means of direct diagonalization calculations with a finite number of single particle modes. The response of the system against a monopolar perturbation is characterized by the moments of the dynamic structure function which are explicitly calculated from the dynamic structure function and by means of sum rules.

## I. INTRODUCTION

Recent experiments with few ultracold atoms trapped in harmonic potentials have opened the way to understand how many-body quantum mechanical correlations build in few-body systems [1–11]. Such systems, if further confined to a 1D geometry, offer an appropriate playground to study the interplay between quantum many-body correlations and statistics. In the present paper, we concentrate in the case of bosons confined in a 1D harmonic oscillator potential and study the behavior of the ground state and collective excitations [9–11].

The simplest example is that of two particles trapped in a harmonic oscillator potential [12]. For the case of a contact interaction potential, which is realistic for most ultracold atomic systems [13], two noteworthy limits are well known. In absence of interactions the two atoms populate the lowest energy single particle state, producing the minimal version of a Bose-Einstein condensed state. In the infinite interaction limit the two bosons resemble in many ways two spinless non-interacting fermions, producing the so called Tonks-Girardeau (TG) limit [14]. The behavior of the two body system in the two limits is completely different [15], reflecting the nature of the quantum correlations between the atoms [16–19]. This behavior can be probed by exciting the trapped two-atom system with the monopolar excitation operator and observing the response. The first collective excitation of the trapped system has the same excitation energy of  $2\hbar\omega$  for both the non-interacting and infinitely interacting limits, being  $\omega$  the trap frequency [20]. This mode has actually two contributions. The first arises from the excitation of the center-of-mass mode. This contribution remains unchanged as we increase the atom-atom interaction and solely depends on the trapping potential. The second contribution is more intricate and corresponds to the first excited mode of the relative motion, e.g. a breathing mode. The excitation energy of this mode changes as we vary the interaction strength. Starting at  $2\hbar\omega$  in the non-interacting case, it decreases

as the atom-atom interaction strength is increased until it reaches a minimum. This increase of the interaction also builds up strong correlations between the two atoms. Past the minimum, the excitation energy increases with the interaction towards its limiting value of  $2\hbar\omega$ , i.e. the same value as the non-interacting case. This reentrance behavior of the breathing mode has been experimentally observed in the case of cesium atoms trapped in very elongated independent tubes (one-dimensional systems) with each tube containing between 8 to 25 atoms at their center [10].

The breathing mode can be excited by varying the trapping potential. That is, for instance, it can be excited by first preparing the system in the ground state corresponding to  $\omega$  and then suddenly quenching the trapping frequency. In Refs. [21, 22] the excitations of the system were studied following this procedure. The excitation energies were obtained from the Fourier analysis of the beating in the system after the quench. Direct diagonalization methods were used in Ref. [23], where the continuum was studied as a limiting case for discrete Bose-Hubbard models. On the other hand, in Ref. [20] quantum Monte-Carlo calculations were performed for systems of up to  $N = 25$  atoms. The method utilized to investigate the breathing mode was to determine the average excitation energy by means of sum rules [24–26], i.e. by computing the expectation value of certain operators in the ground state of the system.

In this article we compute the dynamic structure function (DSF) and study the exact response of the system associated to a monopolar excitation as we vary the atom-atom interaction, which is taken always repulsive. We compare the results obtained by means of the sum rules [16, 24, 25] previously considered [20] with a direct computation integrating the structure function. The article is organized in the following way. In Sec. II we describe the two particle Hamiltonian and explain our diagonalization procedure. In Sec. III we present the dynamic structure function computed at several interaction strengths. Explicit expressions for the sum rules applied

to our system are given in Sec. IV. In Sec. V we provide a summary and the main conclusions of our work. Finally, there is an appendix with some technical details concerning the contribution of the center-of-mass.

## II. HAMILTONIAN

The Hamiltonian for two bosons trapped in a one dimensional harmonic oscillator (h.o.) and interacting through a contact potential reads,

$$H = -\frac{\hbar^2}{2m} \frac{d^2}{dx_1^2} - \frac{\hbar^2}{2m} \frac{d^2}{dx_2^2} + \frac{1}{2}m\omega^2 x_1^2 + \frac{1}{2}m\omega^2 x_2^2 + g\delta(x_1 - x_2). \quad (1)$$

As customary, we can define the center-of-mass (c.m.) and relative coordinates as,  $X = (x_1 + x_2)/2$  and  $x_r = x_1 - x_2$ . This change of variables allows us to decompose the Hamiltonian in two pieces,  $H = H_{c.m.} + H_r$ , with,

$$H_{c.m.} = -\frac{\hbar^2}{2M} \frac{d^2}{dX^2} + \frac{1}{2}M\omega^2 X^2, \\ H_r = -\frac{\hbar^2}{2\mu} \frac{d^2}{dx_r^2} + \frac{1}{2}\mu\omega^2 x_r^2 + g\delta(x_r). \quad (2)$$

where  $M = 2m$  is the total mass and  $\mu = m/2$  is the reduced mass. The frequencies associated to both Hamiltonians are the same. However, the oscillator lengths are different. Now, it is convenient to express the Hamiltonians in the oscillator units of the original Hamiltonian:

$$H_{c.m.} = -\frac{1}{4} \frac{d^2}{dX^2} + X^2, \\ H_r = -\frac{d^2}{dx_r^2} + \frac{1}{4}x_r^2 + g\delta(x_r), \quad (3)$$

where all quantities have been properly re-scaled using the harmonic oscillator units. From now on, we will refer to the  $H_r$  without the interaction term,  $g\delta(x_r)$ , as  $H_r^{(0)}$ .

As the Hamiltonian splits in two commuting ones, the wave functions associated to the c.m. motion and the relative motion factorize,

$$\Psi(X, x_r) = \phi(X) \psi(x_r). \quad (4)$$

$H_{c.m.}$  is a harmonic oscillator Hamiltonian with the spectrum  $E_k^{c.m.} = k + 1/2$  where  $k$  is the number of quanta associated to the c.m. motion.

To diagonalize the relative part we use the following procedure. We choose a finite number of non-interacting energy eigenstates,  $\{\psi_0(x_r), \psi_2(x_r), \dots, \psi_{2M}(x_r)\}$ , corresponding to  $H_r^{(0)}$ . Notice that, in order to fulfil the symmetry requirements of the two-boson wave function, we only consider the modes associated to even functions.

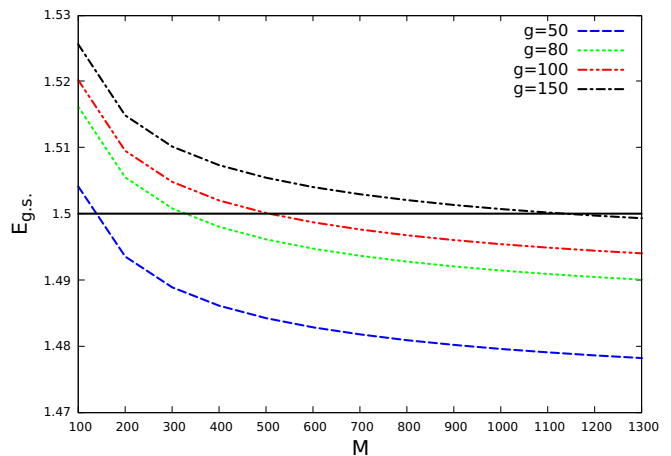


FIG. 1. Ground state energy (in h.o. units) of  $H_r$  as a function of the number of modes (the dimension of the space used to diagonalize the Hamiltonian,  $M$ ) for several values of the interaction strength  $g$ .

Hence, the matrix elements of  $H_r$  are:

$$\langle \Psi_{2m} | H_r | \Psi_{2n} \rangle = \left( \frac{1}{2} + 2n \right) \delta_{m,n} \\ + g \int dx_r \Psi_{2n}(x_r) \Psi_{2m}(x_r) \delta(x_r) \\ = \left( \frac{1}{2} + 2n \right) \delta_{m,n} + g \Psi_{2n}(0) \Psi_{2m}(0). \quad (5)$$

Diagonalizing the truncated Hamiltonian we get approximate solutions, whose eigenvalues are upper bounds of the corresponding exact solutions,

$$H_r \tilde{\Psi}_\ell = \tilde{E}_\ell^{(r)} \tilde{\Psi}_\ell. \quad (6)$$

In practice we use a huge number of modes,  $M$  up to 1500, to guarantee the convergence of the calculations. In fact, in Fig. 1 we report the dependence of the ground state energy on the number of modes used to diagonalize  $H_r$  for different values of the interaction strength  $g$ . Obviously, the energy decreases as the number of modes increases reaching in all cases a limit saturating value with the number of modes which defines an asymptotic value. The horizontal line at  $E_{g.s.} = 3/2$  corresponds to the ground state energy of  $H_r$  in the limit  $g \rightarrow \infty$ . For any finite value of  $g$  one can always find a number of modes ( $M_{crit}$ ) such that for a larger number of modes the energy will be always below  $3/2$ . The  $M_{crit}$  becomes larger as  $g$  increases. Therefore, one can conclude that when  $g \rightarrow \infty$  the ground state energy of  $H_r$ , as a function of the number of modes, approaches  $3/2$  from below.

For the case of two bosons trapped in a harmonic oscillator potential, we could have used the exact solutions of Ref. [12]. Instead, we have decided to present a procedure which, although more tedious for this precise case, is more general and can readily be applied to other single particle trapping potential besides the harmonic oscillator or also to other interactions by a proper computation

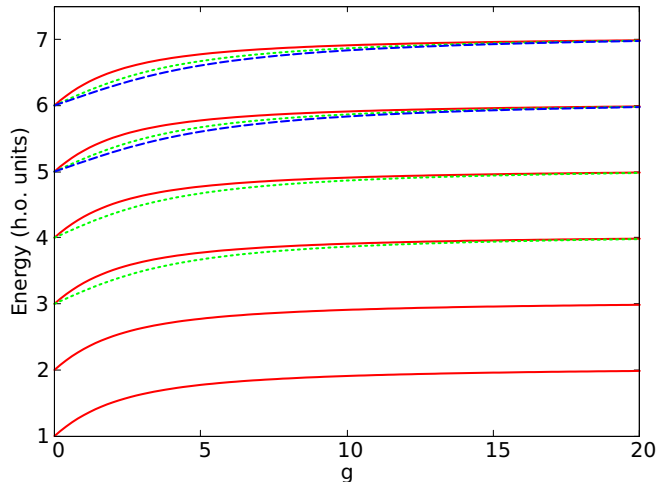


FIG. 2. Lowest energy levels of the spectrum for the two bosons system, for a range of interaction strength  $g = [0, 20]$ . The red lines correspond to the ground state of  $H_r$ , whereas the green and blue lines correspond to 1st and 2nd relative excitations, respectively. These relative Hamiltonian states are also combined with c.m. excitations, which result in parallel curves which are shown with the same color for the same relative Hamiltonian state. For instance, the lowest state takes into account the energy of the ground state of the c.m., equal to  $1/2$  and independent of the strength of the interaction, and the ground state energy of  $H_r$  which is  $1/2$  for  $g = 0$  and approaches  $3/2$  when  $g \rightarrow \infty$ .

of the matrix elements. Our results coincide, when applicable, with the exact solutions of Ref. [12].

Diagonalization methods have also been used for systems with larger number of particles. However, the separation of the problem in c.m. and intrinsic coordinates is more difficult to implement. In those cases, the single-particle wave functions associated to the harmonic trap in the laboratory system are used to build the many-body states of the Fock space. The proper situation of the c.m. excitation modes serves as a test of the size of the Fock space used to diagonalize the Hamiltonian [21, 27, 28].

The full spectrum of the problem will be obtained as,

$$E_{k,\ell} = E_k^{(\text{c.m.})} + \tilde{E}_\ell^{(\text{r})}. \quad (7)$$

In Fig. 2 we depict the lowest part of the spectrum as a function of  $g$ . One can see how the eigenvalues evolve from the non-interacting bosonic system to those of a free fermionic system for  $g \rightarrow \infty$ . At  $g = 0$ , the ground state of  $H$  is non-degenerate. It is built with both atoms in the ground state of the harmonic oscillator single-particle Hamiltonian or, which is the same, as the product of the ground states of  $H_{\text{c.m.}}$  and  $H_r$ . Thus, both descriptions provide the same energy,  $E = 1$ . However, in the  $g \rightarrow \infty$  limit, the ground state of the two-body system is given by the absolute value of the Slater determinant built with one atom in the ground state and the other in the first excited state of the harmonic oscillator single particle Hamiltonian. Therefore, in this limit, the ground state

energy (2 in h.o. units) is the sum of  $1/2$  and  $3/2$  single-particle energies, and the contribution of the contact interaction is zero. When one does the decomposition in  $H_{\text{c.m.}}$  and  $H_r$  the ground state in the  $g \rightarrow \infty$  is achieved by taking the c.m. in the ground state ( $\phi_0(X)$ ), i.e. in the lowest c.m. level with energy  $1/2$ , and taking the relative wave function to be the absolute value of the first excited state,  $\psi_1(x_r)$  of  $H_r^{(0)}$  with energy  $3/2$ . Notice that  $\psi_1(x_r)$  is an odd function and therefore it would be necessary to use an infinite basis of even functions, which are the ones that we have used in the diagonalization of  $H_r$  to respect the symmetry requirements for bosons, to asymptotically approach the exact eigenstate. The lowest excited state of the system corresponds to the first excitation of  $H_{\text{c.m.}}$ , with energy  $3/2$  and to the relative ground state along  $g$ . Thus, the first excited state has a constant excitation energy independent of  $g$ . Actually, the excitations of the c.m. show all the way up resulting in a set of curves parallel to the ground state curve, all depicted with red colour in Fig. 2. Notice that the first excited state at  $g = 0$  can also be described as a properly symmetrized wave function with an atom in the ground state (energy  $1/2$ ) and the other in the first excited state (energy  $3/2$ ) of the single-particle harmonic oscillator Hamiltonian.

The next excitation consists of two states: one corresponds to 2 quanta of excitation of the c.m. motion combined with the ground state of  $H_r$  (red-line); the other one describes the state where the c.m. is in the ground state and the relative motion is in the first excited state of positive parity of  $H_r$  (green line). The two lines coincide at  $g = 0$ , where the energy level has degeneracy 2. Then, as  $g$  increases, the degeneracy is broken (green line) and the energy of this state is always below the energy of the state with two quanta of excitation of the c.m. At  $g \rightarrow \infty$  the two states become again degenerated with total energy 4.

The transition from the BEC regime to the TG regime as the interaction strength is increased is shown in Fig. 3. There, we report as a function of  $g$  the total ground state energy (red line) decomposed in kinetic energy  $E_{\text{kin}}$  (blue line), harmonic oscillator potential energy  $V_{\text{h.o.}}$  (black line) and interaction energy  $V_{\text{int}}$  (green line). We observe that  $V_{\text{h.o.}}$  increases monotonically from  $V_{\text{h.o.}}(g = 0) = 1/2$  up to  $V_{\text{h.o.}}(g \rightarrow \infty) = 1$ , while the kinetic energy starts at  $E_{\text{kin}}(g = 0) = 1/2$  and goes through a minimum before growing up to  $E_{\text{kin}}(g \rightarrow \infty) = 1$ . Notice that both  $E_{\text{kin}}$  and  $V_{\text{h.o.}}$  contain a constant contribution of the c.m. equal to  $1/4$ . We also observe how the interaction energy increases with  $g$  until it reaches a maximum around  $g \simeq 2$ . For  $g \gtrsim 2$  the behavior changes completely and, despite the increasing atom-atom interaction strength, the interaction energy of the ground state decreases monotonically as  $g \rightarrow \infty$ . Notice that, when  $g \rightarrow \infty$ , the exact wave function for the relative motion, built as  $|\psi_1(x_r)|$ , does not feel the interaction. In fact,  $V_{\text{int}}(g = 0) = 0$  and  $V_{\text{int}}(g \rightarrow \infty) = 0$ . This is a clear consequence of the formation of correlations in the sys-

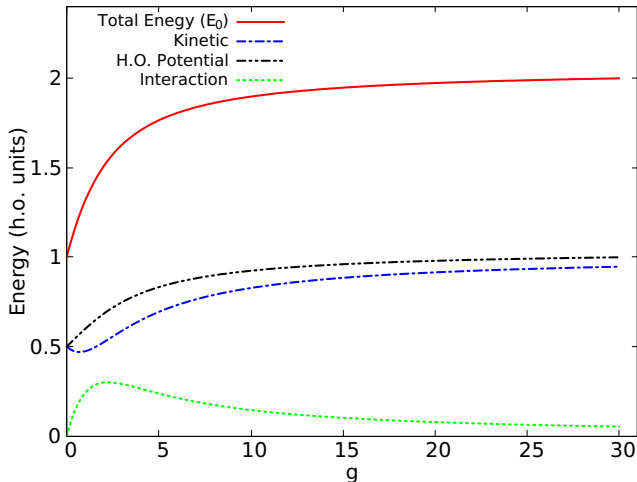


FIG. 3. Different contributors to the ground state energy:  $V_{h.o.}$ ,  $E_{kin}$  and  $V_{int}$ , as functions of the interaction strength  $g$ . The total ground state energy is shown in red,  $E_{kin}$  in blue,  $V_{h.o.}$  in black and  $V_{int}$  in green.

tem which avoid the contact of the two bosons.

Moreover, the virial theorem,

$$-2V_{h.o.} + 2E_{kin} + V_{int} = 0, \quad (8)$$

is exactly fulfilled for any value of  $g$ , indicating a good convergence of the energy results with the number of modes. The virial relation, together with the fact that  $E = E_{kin} + V_{h.o.} + V_{int}$ , allows one to write

$$E_{kin} = \frac{1}{2}E - \frac{3}{4}V_{int}, \quad V_{h.o.} = \frac{1}{2}E - \frac{1}{4}V_{int}. \quad (9)$$

Therefore, we conclude that  $V_{h.o.} \geq E_{kin}$ , for any value of  $g$ . In particular, since  $V_{int} = 0$  at  $g = 0$ ,  $E_{kin} = V_{h.o.} = E/2 = 1/2$ . The same happens at  $g \rightarrow \infty$  when  $V_{int} = 0$ , but now with  $E/2 = 1$ .

In order to understand the behaviour of the different pieces of the energy for very small  $g$ , we can combine a first order perturbation theory with the virial theorem. The correction to the energy is provided by the expectation value  $V_{int,0} = \langle \phi_r^{(0)} | g\delta(x_r) | \phi_r^{(0)} \rangle = g\phi_r^{(0)}(0)\phi_r^{(0)}(0) = g(1/(2\pi))^{1/2}$ , where  $|\phi_r^{(0)}\rangle$  is the ground state of  $H_r^{(0)}$ . Therefore,  $V_{int,0}$  increases linearly with  $g$ . Using the previous relations for  $E_{kin}$  and  $V_{h.o.}$ ,

$$E_{kin} = \frac{1}{2} - \frac{1}{4}V_{int,0} = \frac{1}{2} - \frac{1}{4}g \left( \frac{1}{2\pi} \right)^{1/2}, \quad (10)$$

$$V_{h.o.} = \frac{1}{2} + \frac{1}{4}V_{int,0} = \frac{1}{2} + \frac{1}{4}g \left( \frac{1}{2\pi} \right)^{1/2}. \quad (11)$$

These expressions agree well with the low  $g$  regime depicted in Fig. 3.

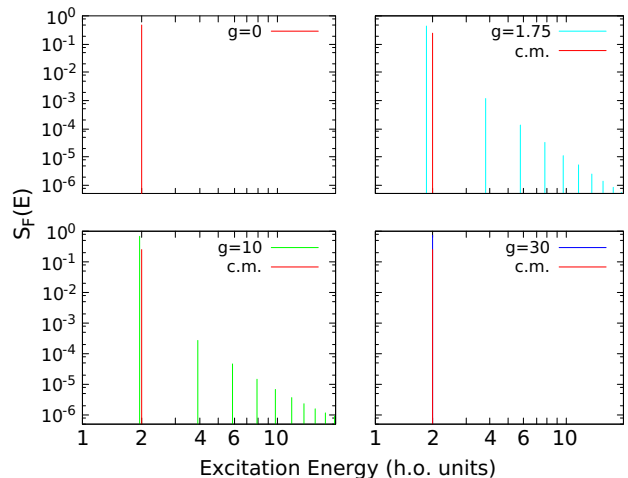


FIG. 4. Dynamic structure function computed for a system composed by 2 bosons, with a delta contact potential. The value is calculated for  $g = 0, 1.75, 10, 30$  and with a number of modes of  $M = 100$ .

### III. DYNAMIC STRUCTURE FUNCTION

The dynamic structure function encodes the response of our system to an external perturbation. In this section we will consider the dynamic structure function of a monopolar excitation, also known as the breathing mode. For a system with an arbitrary number of particles  $N$ , the breathing mode can be excited by the one body operator  $\hat{F} = \sum_{i=1}^N x_i^2$ . Its associated dynamic structure function reads,

$$S_F(E) = \frac{1}{N} \sum_q^D |\langle q | \hat{F} | 0 \rangle|^2 \delta[E - (E_q - E_0)], \quad (12)$$

in which  $D$  is the dimension of the truncated space of the diagonalization and where  $|q\rangle$  runs over the excited states,  $H|q\rangle = E_q|q\rangle$ , and  $|0\rangle$  is the many-body ground state.  $S_F(E)$  can be explicitly computed with the eigenenergies and eigenfunctions of our system. In Fig. 4 we depict the strengths of the dynamic structure function computed with  $N = 2$  for four different values of  $g$ . Notice that they contain the factor  $1/N$  appearing in the definition of  $S_F(E)$ . For  $g = 0$  and  $g \rightarrow \infty$  we can compute  $S_F(E)$  analytically. Notice that the excitation operator  $\hat{F}$  can be split in two pieces (see appendix A), one corresponding to the c.m. and the other to the relative motion. In the case of  $N=2$  it reads:  $x_1^2 + x_2^2 = 2X^2 + x_r^2/2$ . In an experiment, separating the contribution from the c.m. from that of the breathing mode seems involved. The response of the system will thus easily mix both contributions.

For  $g = 0$  the two contributions excite two different states, both at the same excitation energy  $E_{ex} = 2$  ( $E_{ex} = E_q - E_0$ ), being  $1/4$  the strength of the c.m. excitation and  $1/4$  the one of the relative motion.

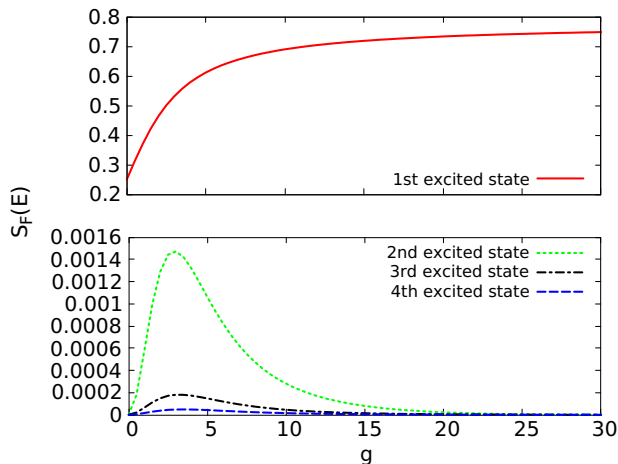


FIG. 5. Strength of the breathing mode (upper panel) and the next three higher relative states excited by the operator  $\hat{F}$  (lower panel) as a function of the interaction strength  $g$ . They contain the factor  $1/N$ .

For nonzero values of  $g$  the DSF is distributed over several excited states. As explained in the appendix A, the c.m. excitation generates only a peak at  $E_{ex} = 2$  with strength  $1/(2N) = 1/4$ , independently of the value of  $g$ . The strength of the breathing mode grows monotonously from  $1/4$  to  $3/4$  as  $g$  increases from 0 to infinity. This implies that even though both excitations have exactly the same energy it should be more likely to excite the breathing mode in the TG limit than in the BEC one. On the other hand, its excitation energy decreases for increasing values of  $g$ , up to  $g \lesssim 2$ . Then, in the  $g \rightarrow \infty$  limit, it reaches again the excitation energy with value  $E_{ex} = 2$ . This reentrant behaviour of the monopolar excitation is reported in Ref. [20]. The strength of the other peaks are always significantly smaller than those of the c.m. and the breathing mode. In Fig. 5 we report the strength of the breathing mode as a function of  $g$  and the strength of the next three excited states of the relative motion. The strength of the breathing mode turns out to be an increasing function of  $g$ . This behaviour will be relevant to understand the evolution of the energy weighted sum rules of  $S_F(E)$ . In all the other cases, the strength is zero for  $g = 0$  and increases with  $g$  up to a maximum, located around  $g \sim 2$ , to decrease again to zero as  $g \rightarrow \infty$ . The maximum decreases when the excitation energy increases. Apparently, this dependence is very much correlated to the dependence of the interaction energy with  $g$  (Fig. 3).

The reentrance behavior affects not only the ground state but also all excited states of the relative motion. As shown in Fig. 6 for several excited states, the reentrance energy, defined as  $E_R = E_{ex}(g) - E_{ex}(g = 0)$ , is zero by definition at  $g = 0$ . For increasing values of  $g$  it goes through a minimum to increase again asymptotically to zero when  $g \rightarrow \infty$ . This reentrance behaviour

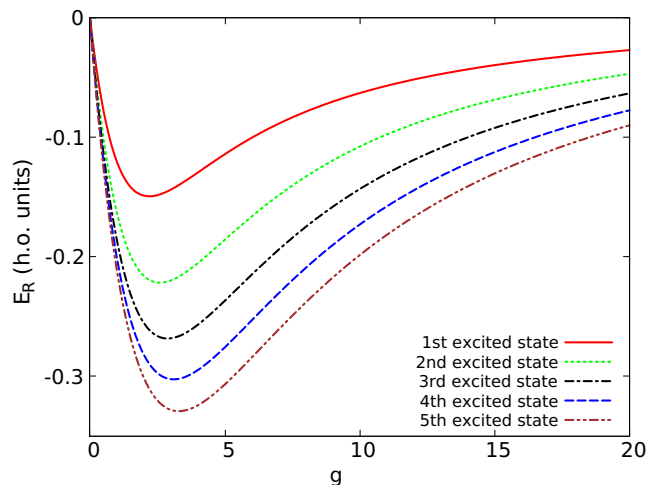


FIG. 6. Reentrance energy,  $E_R = E_{ex}(g) - E_{ex}(g = 0)$  as a function of the interaction strength  $g$  for several excited states of  $H_r$ .

is more pronounced for the higher excited states. The maximum reentrance slightly shifts to higher values of  $g$  for the higher excited states. Again, there seems to exist a correlation between the interaction energy and the reentrance energy as a function of  $g$ .

Computing the structure function explicitly becomes difficult for more than 2 particles. In particular, a naive second quantization scheme using the one particle modes as single particle states runs into difficulties as it mixes the c.m. with the relative motion in a non-trivial way [21]. A way to circumvent this problem would be to consider the excitation operator,  $\hat{F} = \sum_i (x_i - X)^2$ , as in [20].

#### IV. SUM RULES

An alternative method to characterize the dynamic structure function,  $S_F(E)$ , is by calculating its momenta  $M_n$ ,

$$\begin{aligned}
 M_n &= \int_0^\infty E^n S_F(E) dE \\
 &= \frac{1}{N} \sum_q^D (E_q - E_0)^n |\langle q | \hat{F} | 0 \rangle|^2. \quad (13)
 \end{aligned}$$

As it is well known, there are some theorems that allow one to compute several of the  $M_n$  without any explicit knowledge of all the eigenvalues and eigenvectors of the many-body system [24]. This is done through the so-called sum rules. These sum rules will be computed by suitable operations on the ground state of the system.

Also note that the momenta  $n$  and  $n + 2$  provide estimates for the monopolar excitation energy which is how Monte-Carlo calculations proceed [20]. Assuming

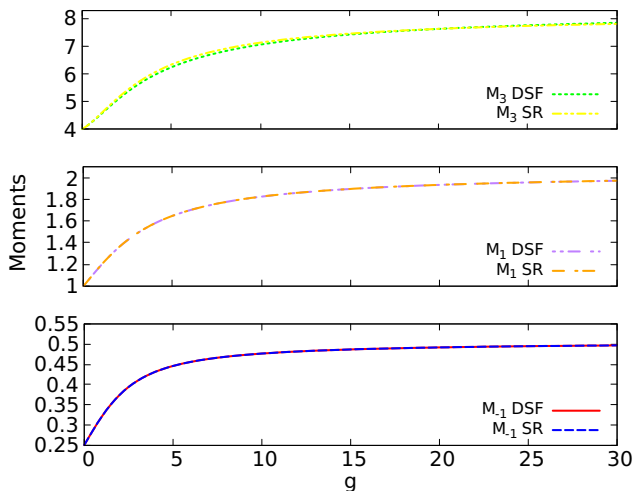


FIG. 7.  $M_{-1}$ ,  $M_1$  and  $M_3$  computed directly from  $S_F(E)$  (DSF) and the sum rules (SR). When using  $S_F(E)$  we have truncated the spectra by taking the first 10 energy levels.

the structure function concentrated around a single excitation energy,  $S_F \simeq S_m \delta(E - E_m)$ , then we have  $E_m \simeq \sqrt{M_n/M_{n-2}}$  for all  $n$ . The simplest one would be  $E_m \simeq \sqrt{M_1/M_{-1}}$ . The sum rules below are derived in full generality, independent of the number of particles of the many body system and, thus, they are particularly useful combined with Monte-Carlo techniques which are able to describe the ground state. However, all the calculations reported in the paper are for  $N = 2$  and have been performed taking into account the separation of the c.m. and the relative motion. The contributions of the c.m. to the considered sum rules are all analytical.

### A. $M_{-1}$ sum rule

To obtain the  $M_{-1}$  sum rule, we build a new Hamiltonian  $\tilde{H} = \hat{H} + \lambda \hat{F}$  and consider the new term as a perturbation modulated by the parameter  $\lambda$ . The expansion up to second order of the ground state energy  $E_0(\lambda)$ , eigenenergy of  $\tilde{H}$ , reads,

$$E_0(\lambda) = E_0 + \lambda \langle 0 | \hat{F} | 0 \rangle + \lambda^2 \sum_q \frac{|\langle q | \hat{F} | 0 \rangle|^2}{E_0 - E_q}, \quad (14)$$

where  $|q\rangle$  and  $E_q$  are eigenstates and eigenvalues of the unperturbed Hamiltonian, respectively. Therefore,  $M_{-1}$  can be written as,

$$M_{-1} = -\frac{1}{2} \frac{1}{N} \left. \frac{\partial^2 E_0(\lambda)}{\partial \lambda^2} \right|_{\lambda=0}. \quad (15)$$

Using also perturbation theory, we have an alternative expression for  $M_{-1}$ ,

$$M_{-1} = -\frac{1}{2} \frac{1}{N} \left. \frac{\partial}{\partial \lambda} \langle \tilde{0} | \hat{F} | \tilde{0} \rangle \right|_{\lambda=0}, \quad (16)$$

where  $|\tilde{0}\rangle$  is the ground state of the perturbed Hamiltonian  $\tilde{H}$ . For the present monopole operator,

$$\frac{1}{N} \langle \tilde{0} | \hat{F} | \tilde{0} \rangle = \frac{1}{N} \langle \tilde{0} | \sum_i x_i^2 | \tilde{0} \rangle = \int_{-\infty}^{\infty} x^2 \rho_\lambda(x) dx, \quad (17)$$

with  $\int_{-\infty}^{\infty} \rho_\lambda(x) dx = 1$ .

### B. $M_1$ sum rule

The  $M_1$  sum rule can be written as,

$$\begin{aligned} M_1 &= \frac{1}{2} \frac{1}{N} \langle 0 | [\hat{F}^\dagger, [\hat{F}, \hat{H}]] | 0 \rangle = 2 \frac{1}{N} \langle 0 | \sum_i x_i^2 | 0 \rangle \\ &= 2 \int_{-\infty}^{\infty} x^2 \rho(x) dx = \frac{4}{N} V_{\text{h.o.}}, \end{aligned} \quad (18)$$

with  $\int_{-\infty}^{\infty} \rho(x) dx = 1$  and  $V_{\text{h.o.}}$  is the total harmonic potential energy.

In Ref. [20] the monopolar excitation energy is estimated by means of  $E \simeq \sqrt{M_1/M_{-1}}$  with  $M_{-1}$  obtained from Eq. (16).

### C. $M_3$ sum rule

Assuming that  $\hat{F}$  is hermitian,  $M_3$  can be calculated as the following expectation value:

$$M_3 = \frac{1}{2N} \langle 0 | [[\hat{H}, \hat{F}], [\hat{H}, [\hat{H}, \hat{F}]]] | 0 \rangle. \quad (19)$$

Alternatively, it can also be calculated as

$$M_3 = \frac{1}{2N} \left. \frac{\partial^2 E_\eta}{\partial \eta^2} \right|_{\eta=0}, \quad (20)$$

where

$$E_\eta = \langle \phi_\eta | \hat{H} | \phi_\eta \rangle \text{ with } |\phi_\eta\rangle = e^{\eta[\hat{H}, \hat{F}]} | 0 \rangle. \quad (21)$$

By means of the virial theorem derived from,

$$\begin{aligned} E_\lambda &= \langle \Psi_\lambda | \hat{H} | \Psi_\lambda \rangle \\ &= \lambda^2 E_{\text{kin}}^{\lambda=1} - \frac{1}{\lambda^2} V_{\text{h.o.}}^{\lambda=1} + \lambda V_{\text{int}}^{\lambda=1}, \end{aligned} \quad (22)$$

with

$$\Psi_\lambda(x_1, x_2, \dots, x_N) \equiv \lambda^{N/2} \Psi(\lambda x_1, \lambda x_2, \dots, \lambda x_N), \quad (23)$$

and noting that

$$e^{\eta[H, F]} \Psi(x_1, x_2, \dots, x_N) = \Psi(e^\eta x_1, e^\eta x_2, \dots, e^\eta x_N), \quad (24)$$

$M_3$  can then be computed as,

$$M_3 = \frac{4}{N} (E_{\text{kin}} + 3V_{\text{h.o.}}). \quad (25)$$

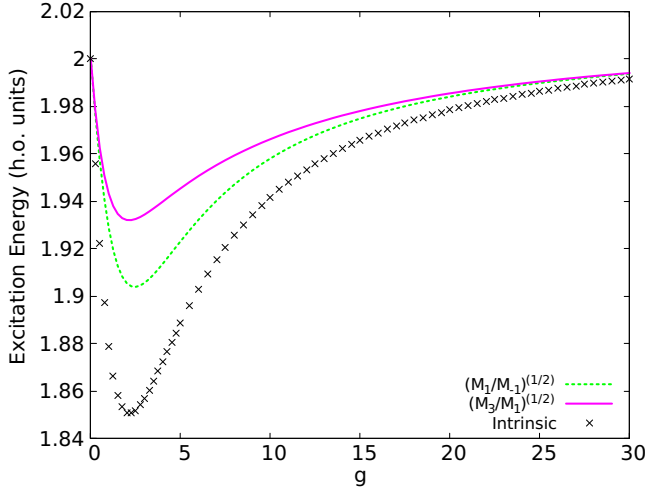


FIG. 8. Monopolar excitation energies obtained through  $M_{-1}$ ,  $M_1$  and  $M_3$ , and first excitation energy from the spectra.

#### D. Behaviour and asymptotic values of the sum rules

In Fig. 7 the sum rules  $M_3$ ,  $M_1$  and  $M_{-1}$  are reported as a function of  $g$ . The sum rules have been calculated by explicitly integrating  $S_F(E)$  or by using the formulas of the sum rules in terms of expectation values of certain operators in the ground state. The agreement between both methods is excellent in the full range of  $g$  explored. All the sum rules are increasing functions of the interaction strength and approach an asymptotic value for  $g \rightarrow \infty$ . The increasing character of the sum rules with  $g$  is mainly due to the increment of the strength of the breathing mode with  $g$ . As expected, the convergence to the asymptotic values is faster for  $M_{-1}$  and slower for  $M_3$ . However, all cases have almost reached convergence already for  $g = 30$ .

As explained in the appendix A, due to the operator  $x_1^2 + x_2^2$  the only excitation of the c.m. lies at an energy  $E_{ex} = 2$ , above the ground state. The strength of this excitation (which contains the factor  $1/N$ ) is  $1/4$  and therefore the contribution to the different sum rules of the c.m. excitation is given by

$$M_{-1,c.m.} = \frac{1}{8}, \quad M_{1,c.m.} = \frac{1}{2}, \quad M_{3,c.m.} = 2. \quad (26)$$

The contributions to the different sum rules of both the energy and the strength of the c.m. excitation are independent of  $g$ .

The non-interacting and the infinitely interacting limits are particularly amenable and allow one to compute the exact limiting values of the  $M_1$  and  $M_3$  sum rules. The two sum rules can be cast as a function of the average values of the kinetic and harmonic oscillator energies.

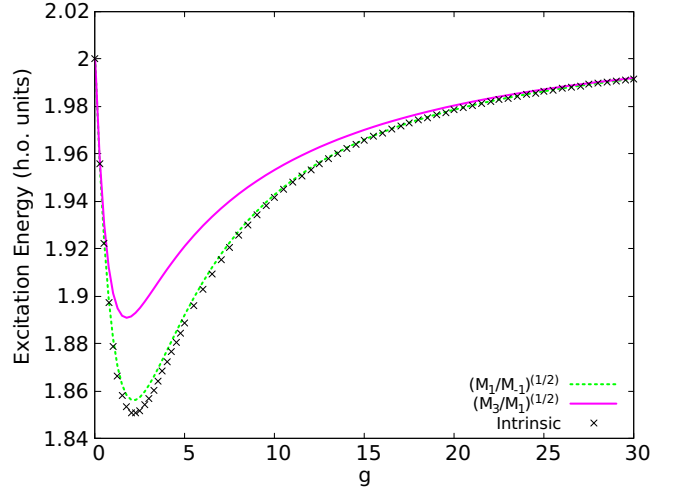


FIG. 9. Monopolar excitation energies obtained through  $M_{-1}$ ,  $M_1$  and  $M_3$ , and the energy of the breathing mode. The contribution of the c.m. to the sum rules has been subtracted.

The  $M_1$  and  $M_3$  sum rules for  $N$  particles read,

$$M_1 = \frac{4}{N} V_{h.o.}$$

$$M_3 = \frac{4}{N} (E_{kin} + 3V_{h.o.}) \quad (27)$$

where  $V_{h.o.}$  is the expectation value of the total harmonic oscillator potential energy in the  $N$ -particle wave function and  $E_{kin}$  is the total kinetic energy associated to the ground state.

For  $g = 0$ , all particles populate the h.o. single-particle ground state. Therefore, the total, kinetic and harmonic potential energies are  $E = N/2$ ,  $E_{kin} = N/4$ , and  $V_{h.o.} = N/4$ , respectively. Hence, for  $N = 2$  we have,  $M_3 = 4$  and  $M_1 = 1$  and the estimate of the monopolar excitation energy characterizing the dynamic structure function  $S_F(E)$  is

$$E_{ex} = \sqrt{\frac{M_3}{M_1}} = 2. \quad (28)$$

To evaluate the sum rules in the limit  $g \rightarrow \infty$  we rely on the Bose-Fermi mapping. In this case, the ground state is the absolute value of the Slater determinant built as if the particles were fermions. In the case of  $N$  particles they occupy the first  $N$  lowest single-particle energy levels of the harmonic oscillator potential so that

$$E = \left( \frac{1}{2} + \frac{3}{2} + \dots + \frac{2N-1}{2} \right) = \frac{1}{2} N^2 \quad (29)$$

while  $E_{kin} = N^2/4$ , and  $V_{h.o.} = N^2/4$ .

Consequently,

$$M_1 = \frac{4}{N} V_{h.o.} = N, \quad M_3 = \frac{4}{N} (E_{kin} + 3V_{h.o.}) = 4N \quad (30)$$

which for  $N = 2$  results in  $M_1 = 2$  and  $M_3 = 8$ . then, the monopolar excitation energy calculated with  $M_3$  and  $M_1$  is, in this case,

$$E_{\text{ex}} = \sqrt{\frac{M_3}{M_1}} = \sqrt{\frac{4N}{N}} = 2, \quad (31)$$

which is the same as in the non-interacting case.

Recalling to Sec.III, the intrinsic motion energy and strength have a dependence on  $g$ , contrary to those of the c.m. excitation. In particular, the strength is an increasing function of  $g$  that goes from  $1/4$  at  $g = 0$  to  $3/4$  at  $g \rightarrow \infty$ . This increment of the strength of the intrinsic peak associated to the monopole vibration is the main reason for the increasing behaviour of the different sum rules as a function of  $g$ . For all values of  $g$ , the peaks associated to the c.m. and to the breathing mode exhaust more than 99% of the sum rules and the other peaks have a marginal influence.

In 1D ultracold gases with atom-atom contact interaction is sensible to neglect the interaction energy in front of the kinetic energy when the interaction strength is increased, unlike in a Thomas-Fermi limit where the kinetic energy is neglected in front of the interaction energy. Therefore, it is also illustrative to compare the  $g \rightarrow \infty$  value with the Thomas-Fermi one, where the kinetic energy is neglected and the estimate of the excitation energy from the sum rules is  $E_{\text{ex}} = \sqrt{3}$ . Thus, as emphasized in [20], the reentrant behavior is a clear consequence of the fermionization taking place as  $g \rightarrow \infty$ . In 1D gases with contact interaction, as the interaction is increased the approximation which is sensible is to neglect the interaction energy in front of the kinetic one, unlike in the Thomas-Fermi limit where the kinetic energy is neglected in front of the interaction.

As the important peaks (c.m. and breathing mode) of  $S_F(E)$  are rather close to each other one expects the estimation of the energy through the sum rules to be rather accurate. In Fig. 8 we compare the monopolar excitation energies estimated by means of the sum rules described above with the values of the excitation energy of the breathing mode,  $E_{0,2} - E_{0,0}$ . Notice that in all cases, the estimate  $\sqrt{M_3/M_1}$  is larger than  $\sqrt{M_1/M_{-1}}$  for any value of  $g$  and both are larger or equal than the minimum excitation energy defined by  $E_{0,2} - E_{0,0}$ . First, we note that the two quantities obtained from  $\sqrt{M_1/M_{-1}}$  and  $\sqrt{M_3/M_1}$  do not produce the same estimate for the intrinsic monopolar excitation energy. This reflects the fact that the structure function contains two relevant excited states not located at the same energy, one from the c.m. and the second from the breathing mode. The difference between the two estimates provided by the sum rules increases with  $g$  and is larger for the value of  $g$  that maximizes the interaction energy. For this value of

$g$  the difference in energy between the c.m. excitation and the energy of the breathing mode is also maximal. Then, when  $g$  increases further and the breathing mode gets closer again to the c.m. excitation, the estimates get closer and both reach asymptotically the  $E_{\text{ex}} = 2$  when  $g \rightarrow \infty$ . Subtracting the contribution of the c.m. to the sum rules, which is equivalent to study only the the intrinsic excitations (see Fig. 9), there is only one dominant peak: the breathing mode, and the estimations from the sum rules get much closer to each other. The differences in this case should be assigned to the higher excitations beyond the breathing mode.

## V. SUMMARY AND CONCLUSIONS

We have considered a system of two bosons trapped in a 1D harmonic oscillator potential. The interaction between the two bosons is assumed to be well represented by a contact term. Under these assumptions we have computed the dynamic structure function for a monopolar excitation as a function of the interaction strength. Our method consists in diagonalizing the Hamiltonian of the relative motion in a large enough truncated basis. In this way we are able to obtain stable results for both the positions and strengths of the peaks of the dynamic structure function. We have compared the direct calculation of the lower momenta of the dynamic structure function with computations performed by means of sum rules. The agreement between both methods is almost perfect for  $M_{-1}$  and  $M_1$ , and is within 2% check this percentage for  $M_3$ . We have computed two estimates of the monopolar excitation energy obtained from  $\sqrt{M_1/M_{-1}}$  and  $\sqrt{M_3/M_1}$ . Differences between both estimates reflect the fact that a minimum of two peaks (c.m. and breathing mode) are always contributing to the structure function for any value of  $g$ . When the c.m. contribution is subtracted from the sum rules, the prediction of the excitation energy of the intrinsic breathing mode improves substantially. Finally, as shown in the appendix, the contribution of the c.m. to the sum rules decreases with the number of particles. Therefore, it is expected that the sum rule approach to estimate the monopole excitation will work better for a larger number of particles.

## ACKNOWLEDGMENTS

The authors acknowledge useful discussions with Joan Martorell and Miguel Angel García March. We acknowledge financial support from the Spanish Ministerio de Economía y Competitividad Grant No FIS2017-87534-P, and from Generalitat de Catalunya Grant No. 2014SGR401.

[1] X. He, P. Xu, J. Wang, and M. Zhan, Opt. Express **18**, 13586 (2010).

[2] F. Serwane, G. Zürn, T. Lompe, T. B. Ottenstein, A. N. Wenz, and S. Jochim, Science **332**, 336 (2011).



- [3] G. Zürn, F. Serwane, T. Lompe, A. N. Wenz, M. G. Ries, J. E. Bohn, and S. Jochim, *Phys. Rev. Lett.* **108**, 075303 (2012).
- [4] A. N. Wenz, G. Zürn, S. Murmann, I. Brouzos, T. Lompe, and S. Jochim, *Science* **342**, 457 (2013).
- [5] R. Bourgain, J. Pellegrino, A. Fuhrmanek, Y. R. P. Sortais, and A. Browaeys, *Phys. Rev. A* **88**, 023428 (2013).
- [6] G. Pagano, M. Mancini, G. Cappellini, P. Lombardi, F. Schäfer, H. Hu, X.-J. Liu, J. Catani, C. Sias, M. Inguscio, and L. Fallani, *Nat. Phys.* **10**, 198 (2014).
- [7] S. Murmann, A. Bergschneider, V. M. Klinkhamer, G. Zürn, T. Lompe, and S. Jochim, *Phys. Rev. Lett.* **114**, 080402 (2015).
- [8] A.M. Kaufman, B.J. Lester, M. Foss-Feig, M.L. Wall, A.M. Rey, and C.A. Regal, *Nature* **527**, 208 (2015).
- [9] H. Moritz, T. Stoferle, M. Köhl, and T. Esslinger, *Phys. Rev. Lett.* **91**, 250402 (2003).
- [10] E. Haller, M. Gustavsson, M.J. Mark, J.G. Danzl, R. Hart, G. Pupillo, and H.-C. Nägerl, *Science* **325**, 1224 (2009).
- [11] B. Fang, G. Carleo, A. Johnson, and I. Bouchoule, *Phys. Rev. Lett.* **113**, 035301 (2014).
- [12] T. Busch, B-G. Englert, K. Rzazewski, and M. Wilkens, *Found. Phys.* **28**, 549 (1998).
- [13] F. Dalfovo, S. Giorgini, L. Pitaevskii, and S. Stringari, *Rev. Mod. Phys.* **71**, 463 (1999).
- [14] M. Girardeau, *J. Math. Phys.* **1**, 516 (1960).
- [15] Z. Idziaszek and T. Calarco, *Phys. Rev. A* **74**, 022712 (2006).
- [16] S. Stringari, *Phys. Rev. Lett.* **77**, 2360 (1996).
- [17] S. Zöllner, H.-D. Meyer and P. Schmelcher, *Phys. Rev. A* **74**, 063611 (2006).
- [18] L. M. A. Kehrberger, V. J. Bolsinger and P. Schmelcher, *Phys. Rev. A* **97**, 013606 (2018).
- [19] I. Brouzos, and P. Schmelcher, *Phys. Rev. Lett.* **108**, 045301 (2012).
- [20] A. Iu. Gudyma, G. E. Astrakharchik, Mikhail B. Zvonarev, *Phys. Rev. A* **92**, 021601 (2015).
- [21] R. Schmitz, S. Krönke, L. Cao and P. Schmelcher, *Phys. Rev. A* **88**, 043601 (2013).
- [22] M. Pyzh, S. Krönke, C. Weitenberg, and P. Schmelcher, *New J. Phys.* **20**, 015006 (2018).
- [23] W. Tschischik, R. Moessner, and M. Haque, *Phys. Rev. A* **88**, 063636 (2013).
- [24] O. Bohigas, A. M. Lane, and J. Martorell, *Phys. Rep.* **51**, 267 (1979).
- [25] C. Menotti and S. Stringari, *Phys. Rev. A* **66**, 043610 (2002).
- [26] J. W. Abraham and M. Bonitz, *Contrib. Plasma Phys.* **54**, 27 (2014).
- [27] M. A. Garcia-March, B. Juliá-Díaz, G.E. Astrakharchick, T. Busch, J. Boronat, and A. Polls, *Phys. Rev. A* **88**, 063604 (2013).
- [28] F. Deuretzbacher, K. Bongs, K. Sengstock, and D. Pfannkuche, *Phys. Rev. A* **75**, 013614 (2007).

## Appendix A: Center-of-mass for N-particles and its monopolar excitation

An interesting feature of this two-body problem is the relation between the many-body correlations and the monopolar excitation in the system. In any experimental implementation it will be difficult, if not impossible, to separate the center-of-mass (c.m.) contribution from the internal one, which is the one carrying information about the correlations. Notably, for an arbitrary number of particles, the c.m. contribution can be evaluated analytically.

Lets start from the following identity,

$$\sum_{i=1}^n x_i^2 = NX^2 + \frac{1}{N} \sum_{i<j} (x_i - x_j)^2. \quad (\text{A1})$$

and consider an  $N$ -particle Hamiltonian with interactions depending on the interparticle distance, confined in a harmonic oscillator potential,

$$H = - \sum_{i=1}^N \frac{1}{2} \frac{d^2}{dx^2} + \frac{1}{2} \sum_{i=1}^N x_i^2 + \sum_{i<j} v(x_i - x_j). \quad (\text{A2})$$

Which can be decomposed in two pieces,

$$H = H_{\text{c.m.}} + H_r \quad (\text{A3})$$

where  $H_{\text{c.m.}}$ :

$$H_{\text{c.m.}} = - \frac{1}{2N} \frac{d^2}{dX^2} + \frac{N}{2} X^2 \quad (\text{A4})$$

describes the c.m. motion and  $H_r$  affects only the relative coordinates and is translationally invariant. Notice that for  $N = 2$ , we recover the c.m. Hamiltonian of the two particle case, Eq. (3). Therefore the many-body wave functions of the system can be factorized,

$$\Psi_j(x_1, x_2, \dots, x_n) = \varphi_{j_{\text{c.m.}}}(X) \phi_{j_r}(\{x_i^r\}). \quad (\text{A5})$$

Let's now go back to the definition of the dynamic structure function:

$$S_F(E) = \frac{1}{N} \sum_j \left| \langle j | \sum_{i=1}^N x_i^2 | 0 \rangle \right|^2 \delta(E - (E_j - E_0)), \quad (\text{A6})$$

which can also be separated in a piece corresponding to the center-of-mass an another piece affecting only the relative coordinates:

$$\begin{aligned} \langle j | \sum_i x_i^2 | 0 \rangle &= \\ \langle j_{\text{c.m.}}, j_r | NX^2 + \frac{1}{N} \sum_{i<j} (x_i - x_j)^2 | 0_{\text{c.m.}}, 0_r \rangle & \end{aligned} \quad (\text{A7})$$

where  $|0, 0\rangle = \varphi_0^{\text{c.m.}}(X) \phi_0^r(\{x_i^r\})$ ,

$$\begin{aligned} \langle j | \sum_i x_i^2 | 0 \rangle &= \langle j_{\text{c.m.}} | NX^2 | 0_{\text{c.m.}} \rangle \langle j_r | 0_r \rangle \\ &+ \langle j_{\text{c.m.}} | 0_{\text{c.m.}} \rangle \langle j_r | \frac{1}{N} \sum_{i<j} (x_i - x_j)^2 | 0_r \rangle. \end{aligned} \quad (\text{A8})$$

Taking into account the orthogonality of the states,

$$\begin{aligned} \langle j | \sum_i x_i^2 | 0 \rangle &= \langle j_{\text{c.m.}} | NX^2 | 0_{\text{c.m.}} \rangle \delta_{j_r, 0_r} \\ &+ \delta_{j_{\text{c.m.}}, 0_{\text{c.m.}}} \langle j_r | \frac{1}{N} \sum_{i<j} (x_i - x_j)^2 | 0_r \rangle. \end{aligned} \quad (\text{A9})$$

Therefore, we have separated the excitations of the c.m. from the intrinsic ones. Now, we should take into account that the spectrum of the c.m. is indential to the harmonic oscillator:  $1/2, 3/2, 5/2, \dots$  and that the ground state will correspond always to the  $j_{\text{c.m.}} = 0$  state with energy  $1/2$ . With this excitation operator, the only excitation of the c.m. will correspond always to excite the state  $j_{\text{c.m.}} = 2$  with energy  $E^{\text{c.m.}} = 5/2$ , with an excitation energy  $E_{ex}^{\text{c.m.}} = 2$ . The matrix element, for  $j_{\text{c.m.}} \neq 0$  fulfils that:

$$\langle j_{\text{c.m.}} | NX^2 | 0_{\text{c.m.}} \rangle = \delta_{j_{\text{c.m.}}, 2} N \langle 2_{\text{c.m.}} | X^2 | 0_{\text{c.m.}} \rangle. \quad (\text{A10})$$

Actually, one can evaluate this matrix element:

$$\langle 2_{\text{c.m.}} | X^2 | 0_{\text{c.m.}} \rangle = \frac{1}{\sqrt{2}N} \quad (\text{A11})$$

and

$$\left| \langle 2_{\text{c.m.}} | NX^2 | 0_{\text{c.m.}} \rangle \right|^2 = \left| N \frac{1}{\sqrt{2}N} \right|^2 = \frac{1}{2}. \quad (\text{A12})$$

Therefore, the c.m. excitation appears always at an excitation energy  $E_{ex} = 2$  with strength  $1/(2N)$ , independently of the interactions between the particles. The factor  $1/N$  is due to our definition of  $S_F(E)$ .

### 1. Contribution of the c.m. excitations to the different sum rules

We have shown that the only excitation of the c.m. due to  $F = \sum x_i^2$  lies at an energy  $E_{ex} = 2$ , above the ground state, independently of the interaction between the particles. The strength of this excitation is given by  $1/2N$ . Contributions of this c.m. excitation to the energy weighted sum rules:

$$\begin{aligned} M_{-1, \text{c.m.}} &= \frac{1}{E_{ex}} \frac{1}{N} \frac{1}{2} = \frac{1}{4N} \\ M_{1, \text{c.m.}} &= E_{ex} \frac{1}{N} \frac{1}{2} = \frac{1}{N} \\ M_{3, \text{c.m.}} &= E_{ex}^3 \frac{1}{N} \frac{1}{2} = \frac{4}{N} \end{aligned} \quad (\text{A13})$$

that for  $N = 2$  become:

$$M_{-1, \text{c.m.}} = \frac{1}{8}, \quad M_{1, \text{c.m.}} = \frac{1}{2}, \quad M_{3, \text{c.m.}} = 2. \quad (\text{A14})$$

These results can be always used as a test for the calculations.